Deep Learning Diagnostic Tools for Digital Chemical Pathology

Akshat K. Shahi[a,b], Chathurya Devineni[a,c], Peter W. Hsu[a,c], Kianoush Falahkheirkhah[a], Rohit Bhargava[a,c,d,e,f,g]

[a] Beckman Institute for Advanced Science and Technology, University of Illinois Urbana-Champaign; [b] Siebel School of Computing and Data Science, [c] Departments of Bioengineering, [d] Chemical and Biomolecular Engineering, [e] Electrical and Computer Engineering, [f] Mechanical Science and Engineering, Grainger College of Engineering, University of Illinois Urbana-Champaign; [g] Cancer Center at Illinois, University of Illinois Urbana-Champaign

CISL chemimage.illinois.edu CHEMICAL IMAGING AND STRUCTURES LABORATORY

ILLINOIS Beckman Institute for Advanced Science & Technology

Motivation

Conventional pathology is labor-intensive and time-consuming, involving tissue preparation, staining of biopsy material, and manual microscopic review, often stretching turnaround to several days between the initial biopsy and the diagnostic report. Leveraging deep learning with label-free infrared (IR) imaging offers a streamlined, faster workflow that can reduce delays while improving the quality and consistency of histologic assessment [1–3].

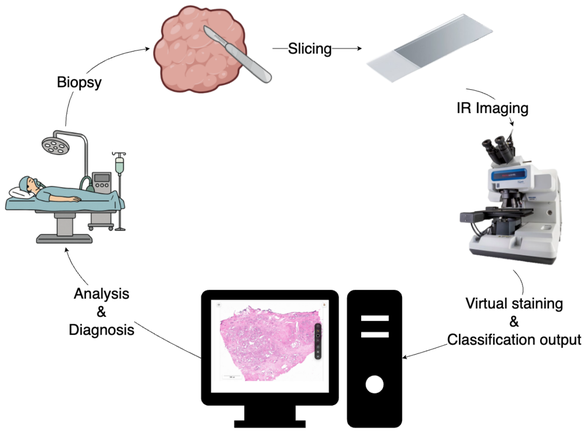

Deep learning (DL) algorithms can be trained to transform IR images into common stains for fast, label-free pathology. This virtual staining approach uses the chemical contrast provided by mid-IR absorption and converts this data into a human-readable form. DL algorithms can associate IR spectral characteristics with cancer pathologies, enabling the automation of repetitive diagnostic tasks.

Sample Preparation & Imaging

Unstained human tissue specimens from Mayo Clinic (Rochester, MN) were first imaged on our custom-designed infrared (IR) microscope with co-registered darkfield (DF) imaging prior to any staining. The same sections were then stained with Hematoxylin and Eosin (H&E). Post-stain brightfield whole-slide images were acquired, stain normalization was applied, and all modalities (IR, DF, H&E) were spatially registered. The pre-stain IR (± DF) data served as input for virtual staining to generate synthetic H&E images. Ground-truth annotations of cancerous regions were produced by board-certified pathologists using the corresponding real H&E slides as reference.

Automated CK Detection for Lymph Node

Dataset

Biopsies of endometrial lymph node tissue were used for model training and dataset development. IR and DF images were the inputs. Because cytokeratin (CK) expression marks metastatic epithelial (CK+) foci in lymph node, CK IHC slides from parallel sections were used to guide precise CK+ vs CK– annotations. 22 whole slide images (WSIs) were used for training/validation and 3 WSIs were held out for test. All images were downsampled to 4.57 µm/pixel, normalized to the dataset mean and standard deviation, and augmented with random flips and transposes.

Architecture

An Attention U-Net model [4] with cross entropy loss was used to train the segmentation model for the lymph node dataset. Incorporating an attention mechanism into the U-Net helps enhance feature extraction by reducing activation on irrelevant regions in the skip connections.

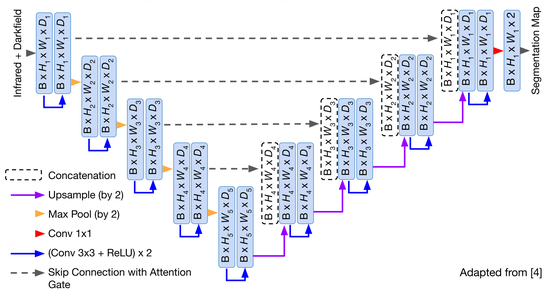

Results

The first row of the following figure shows successful cancer detection while the second row shows a case of model failure. The model had a validation F1-score (%) of 99.97 and 93.59 for non-cancer and cancer regions, respectively.

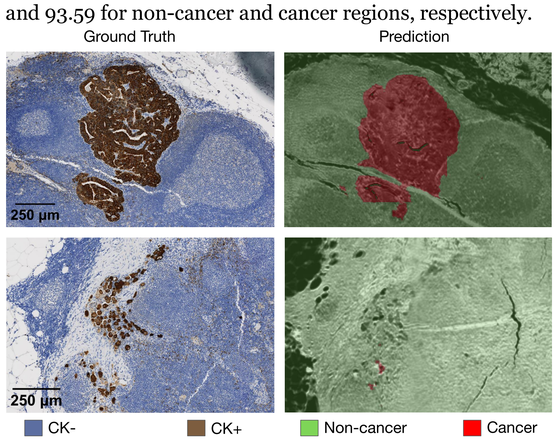

Discussion

The Attention U-Net model can reasonably detect large areas of cancer but has trouble detecting smaller areas of cancer. In future iterations, we want to add annotations and experiment with different training methods such as transfer learning and multitask learning.

Knowledge Distillation for Prostate Cancer Segmentation

Dataset

Prostate biopsies were used for model training and dataset development. IR and DF images were the inputs. 30 WSIs were used for training, 3 for validation, and 18 were held out for test. All images were downsampled to 6 µm/pixel, normalized to the training dataset mean and standard deviation, and augmented with random flips and rotations.

Architecture

A knowledge distillation architecture comprised of identical student and teacher Attention U-Nets was developed to improve the performance of segmentation.

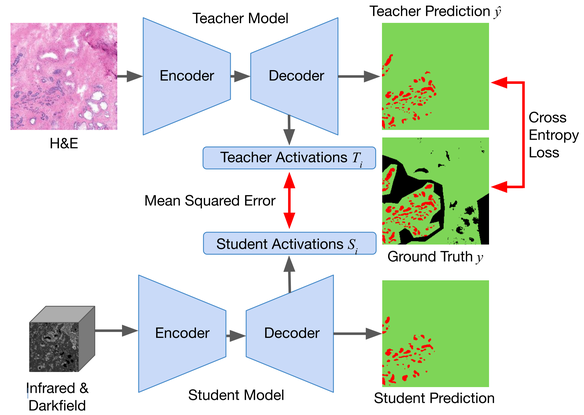

$$\mathcal{L}_{teacher} = CE(\hat{y}, y) \qquad \mathcal{L}_{student} = \sum_{i=0}^{n} w_i * MSE(T_i, S_i)$$

Results

Our knowledge distillation model resulted in increased detection of cancerous regions compared to the baseline single Attention U-Net. The baseline had a test F1-score of 67.67, whereas our approach achieved a F1-score of 70.97.

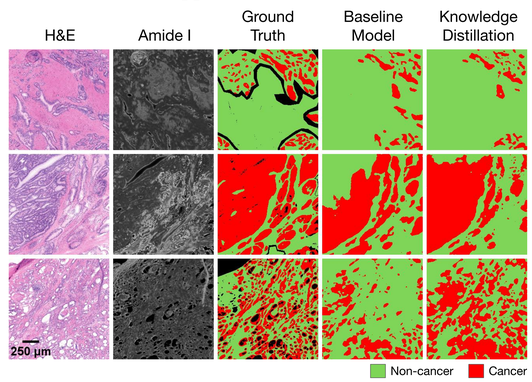

Discussion

Knowledge distillation has the potential to improve segmentation results compared to using a single model. Detection of cancerous regions increased but precise shapes are not yet predicted by the models.

Virtual Staining

DF and IR images of unstained tissue are not diagnosable by pathologists, so we use Virtual Staining to transform them into virtual H&E images. This is done using a ResNet50-based U-Net with CBAM attention.

Speed Optimizations

For IR-based virtual staining to enhance traditional histopathology, it must be accurate, rapid, and diagnostically actionable.

Inference and image processing were done on a Dell Precision 7960 workstation with an Intel Xeon w7-3455 and Nvidia A4500 GPU. After extensive testing, we ended up with two solutions that provided consistent inference time improvement with no loss in output quality.

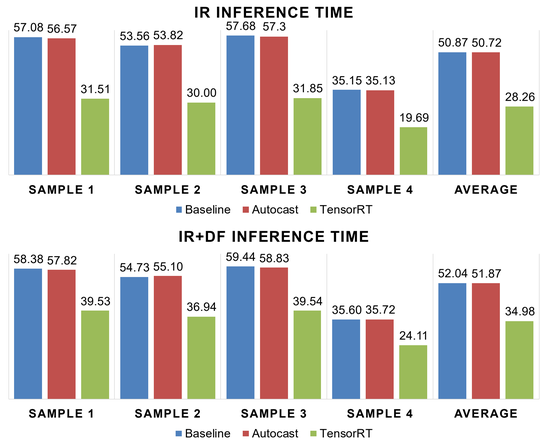

Autocast is a PyTorch feature that enables faster inference by reducing some tensor operations to floating point 16 (fp16). Converting the model to TensorRT takes reduced precision optimization further with the addition of layer and tensor fusion. Model conversion took 533.02s (IR) and 525.70s (IR+DF), which is a one-time development cost.

Discussion

The reduction in inference time post-conversion is significant, and TensorRT will be used in the pipeline. Currently, DF and IR data are stored in 2 separate files. In the future, establishing a format that can store both data types in a single file will reduce the number of read operations and the end-to-end time. Additionally, we hope to expand virtual staining to other types of stains.

Acknowledgements & References

Supported in part by the National Institutes of Health grant R01CA260830, the National Science Foundation grant 1725729, and the University of Illinois Urbana-Champaign. We thank Ji Hun Oh and Dou Hoon Kwark for guidance.

[1] K. Yeh et al., "Infrared spectroscopic laser scanning confocal microscopy for whole-slide chemical imaging," *Nat Commun*, vol. 14, no. 1, p. 5215, Aug. 2023, doi: 10.1038/s41467-023-40740-w.

[2] K. Falahkheirkhah et al., "Accelerating Cancer Histopathology Workflows with Chemical Imaging and Machine Learning," *Cancer Research Communications*, vol. 3, no. 9, pp. 1875–1887, Sep. 2023, doi: 10.1158/2767-9764.CRC-23-0226.

[3] K. Falahkheirkhah, K. Yeh, S. Mittal, L. Pfister, and R. Bhargava, "Deep learning-based protocols to enhance infrared imaging systems," *Chemometrics and Intelligent Laboratory Systems*, vol. 217, p. 104390, Oct. 2021, doi: 10.1016/j.chemolab.2021.104390.

[4] O. Oktay et al., "Attention U-Net: Learning Where to Look for the Pancreas," in *1st Conference on Medical Imaging with Deep Learning*, Amsterdam, The Netherlands, Jul. 2022.